Dynamic PET Denoising Incorporating a Composite Image Guided Filter

Lijun Lu, Debin Hu, Xiaomian Ma, Jianhua Ma, *Member, IEEE,* Arman Rahmim, *Senior Member, IEEE,* and Wufan Chen*, *Senior Member, IEEE*

***Abstract*–We proposed a composite image guided filtering technique for dynamic PET denoising to enable quantitatively enhanced time frames. The guided filter computes the filtering output by considering the content of a guidance image, which can be the input image itself or a different image. In this paper, the composite image from the entire time series is considered as the guidance image. Thus, a local linear model is established between the composite image and individual PET time frames. Subsequently, linear ridge regression is exploited to derive an explicit composite image guided filter. For validation, 20 minute FDG PET data from a NEMA NU 4-2008 IQ phantom were acquired in the list-mode format via the Siemens Invoen micro PET, and were subsequently divided and reconstructed into 20 frames. We compared the performances (including visual and quantitative profiles) of the proposed composite image guide filter (CIGF) with a classic Gaussian filter (GF), and a highly constrained back projection (HYPR) filter. The experimental results demonstrated the proposed filter to achieve superior visual and quantitative performance without sacrificing spatial resolution. The proposed CIGF is considerably effective and has great potential to process the data with high noise for dynamic PET scans.**

I. Introduction

Positron emission tomography (PET) is a powerful *in vivo* molecular imaging modality enabling measurements of radiotracer distributions [1]. Typically, dynamic scans are performed to measure quantitative changes over time with subdivision of data into shorter frames. The use of increasingly short frames enables higher temporal sampling at the expense of amplified signal-to-noise ratios (SNRs) in each image. Thus, the use of kinetic modeling will result in very noisy parametric images, which limit the clinical application of dynamic PET.

Traditionally, standard dynamic PET imaging consists of independent image reconstruction at individual frames followed by application of kinetic model to the time activity curves (TAC) at the voxel or ROI level. Independent image reconstruction is commonly accomplished using statistical image reconstruction methods, such as maximum likelihood (ML) method [2]. However, direct ML estimates of PET images exhibit high variance at low counts [3]. This problem of low counts is further accentuated with increased temporal sampling. Bayesian methods attempt to tackle this ill-posedness in PET image reconstruction through the incorporation of prior models, such as spatial priors (e. g. Huber [4], Nuyts [5]) and anatomical priors (e. g. Bowsher [6] and Joint prior [7]). In particular, 4D reconstruction strategies exploit the spatiotemporal correlation in dynamic PET scans to improve the accuracy of parameter estimation. However, 4D reconstruction methods can be algorithmically and computationally intensive and require further optimization efforts [8].

In contrast to 4D reconstructions, our group proposed a 3.5D dynamic PET reconstruction incorporating kinetic-based clusters via clustering preliminary reconstructed dynamic images to define clustered neighborhoods of voxels with similar kinetics [9]. Wang and Qi proposed a dynamic PET image reconstruction using kernel method, where the kernel matrix is learned from the preliminary reconstructed 3 20-minute frames. The kernel matrix was used to reconstruct the original 24 time frames individually [10]. Both of these methods exploit the preliminary reconstructed images to derive the relationship of different voxels.

Besides the image reconstruction-based methods, post-reconstruction strategies process the time series data reconstructed with filtered back projection (FBP) or ordered-subset expectation maximization, thus being more readily applicable to clinical data. The highly constrained back-projection (HYPR) was originally designed in magnetic resonance imaging (MRI) for image reconstruction from sparse sampled data [11], where the composite image prior was used to improve the reconstructed image quality. The HYPR method was also applied to dynamic PET images denoising [12] and the optimized HYPR-LR was developed for improving the kinetic parameter estimation [13].

Recently, He *et al.* proposed a guided filter, which generates filtering output by considering the content of a guidance image [14, 15]. Inspired by it, we proposed a composite image guided filtering technique for dynamic PET denoising to enable quantitatively enhanced time frames. In this paper, the composite image from the entire time series is considered as the guidance image. Thus, a local linear model

Manuscript received November 26, 2014. This work was supported by the Specialized Research Fund for the Doctoral Program of Higher Education under grant 20134433120017, the Medical Scientific Research Foundation of Guangdong Province under grant B2014240, and the National Natural Science Foundation of China under grants 11205081.

L. Lu (e-mail: ljlubme@gmail.com), D. Hu (e-mail: hdb1991a2012@gmail.com), X. Ma (e-mail: maxiaomian123@gmail.com), J. Ma (e-mail: jhma75@gmail.com), and W. Chen* (e-mail: chenwf@fimmu.com) are with the Guangdong Provincial Key Laboratory of Medical Image Processing and School of Biomedical Engineering, Southern Medical University, Guangzhou, Guangdong, China.

A. Rahmim (e-mail: arahmim1@jhmi.edu) is with the Department of Radiology and Department of Electrical & Computer Engineering, Johns Hopkins University, Baltimore, MD, USA.

is established between the composite image and individual PET time frames. Subsequently, linear ridge regression is exploited to derive an explicit composite image guided filter. Using clinical physics phantom data, we compared the performances of the proposed composite image guide filter (CIGF) with a classic Gaussian filter (GF), and a highly constrained back projection (HYPR) filter. The experimental results demonstrated the proposed filter to achieve superior visual and quantitative performance without sacrificing spatial resolution. The proposed CIGF is considerably effective and has great potential to process the data with high noise for clinical dynamic PET scans.

II. Materials and Methods

A. Guided filter

The key assumption of the guided filter is a local linear model between the guidance I and the filtering output q [4]. We denote that the output image q as a linear transformation of the guidance image I in a spatial window ω_k centered at voxel k :

$$q_i = a_k I_i + b_k, \forall i \in \omega_k, \tag{1}$$

where (a_k, b_k) are the constant or linear coefficients that map I_i to q_i in the spatial window ω_k. If we define the filtering input p, then the following constrain is derived:

$$n_i = p_i - q_i, \tag{2}$$

where n is the difference image between the noisy input image p and the filtered output image q. To determine the linear coefficients (a_k, b_k), we should minimizes the difference between p and q, while maintaining the local linear model (1). Thus, we can minimize the following cost function in window ω_k,

$$E(a_k, b_k) = \sum_{i \in \omega_k} ((a_k I_i + b_k - p_i)^2 + \varepsilon a_k{}^2), \tag{3}$$

where ε is a regularization parameter controlling the range of a_k. Then the solution can be arrived at by linear ridge regression [16] and is given by:

$$a_k = \frac{\frac{1}{|\omega|}\sum_{i \in \omega_k} I_i p_i - \mu_k \bar{p}_k}{\sigma_k^2 + \varepsilon}, \tag{4}$$

$$b_k = \bar{p}_k - a_k \mu_k. \tag{5}$$

Noting that μ_k and σ_k^2 are the mean and variance of the guidance I in ω_k, respectively. $|\omega|$ is the total number of voxels in ω_k, $\bar{p}_k = \frac{1}{|\omega|}\sum_{i \in \omega_k} p_i$ is the mean of input noisy image in ω_k. Thus, the output image q can be represented as:

$$q_i = \frac{1}{|\omega|}\sum_{k | i \in \omega_k} (a_k I_i + b_k) = \bar{a}_i I_i + \bar{b}_i. \tag{6}$$

Here, $\bar{a}_i = \frac{1}{|\omega|}\sum_{k \in \omega_i} a_k$ and $\bar{b}_i = \frac{1}{|\omega|}\sum_{k \in \omega_i} b_k$ are the average coefficient of all windows overlapping i. Based on Eq. (4-6), the filter output q at a pixel i is expressed as a weighted average given by [14, 15]:

$$q_i = \sum_j W_{ij}(I) p_j \tag{7}$$

where the kernel weight is

$$W_{ij}(I) = \frac{1}{|\omega|^2}\sum_{k:(i,j) \in \omega_k} (1 + \frac{(I_i - \mu_k)(I_j - \mu_k)}{\sigma_k^2 + \varepsilon}). \tag{8}$$

B. Composite image guided filter (CIGF)

In our dynamic PET imaging application, the reconstructed individual frame can be expressed as I^t, $t = 1, 2, \cdots, T$. The composite image of the individual frames can be expressed as follows:

$$I^c = f(I^t) \tag{9}$$

where f is the composite operator, the simplest form can be sum of all the individual frames $I^c = \sum_{t=1}^{T} I^t$. Therefore, I^c was served as guidance image, which represented the entire summed PET dynamic images. For each of the dynamic frame I^t, the filter output Q^t is derived as follows:

$$Q_i^t = \sum_j W_{ij}(I^c) I_j^t. \tag{10}$$

Thus, we defined a composite image guide filter for dynamic PET images. Note that others form of I^c also can be considered, as in [10, 13].

C. PET Data Acquisition

A NEMU NU4-2008 IQ phantom was filled with a 18.54MBq ^{18}F-FDG, and scanned using small animal Invoen PET, as we had elaborated in [17], in Nanfang Hospital, Southern Medical University, Guangzhou, China. The phantom contained holes (diameters, 0.8, 1.0, 1.25, 1.5, 2.0, and 2.5 mm) arranged in wedged-shaped groupings, with the center-to-center hole separation being twice the hole diameter. The dynamic data were acquired 20 minutes in the list-mode format and were subsequently divided and reconstructed into 20 frames with dimensions of $256 \times 256 \times 159$, and $0.39 \times 0.39 \times 0.79$ mm^3.

D. Evaluation Metrics

The images were reconstructed using the FBP method and filtered using Gaussian filtering (GF), HYPR approach and composite image guided filtering (CIGF) respectively. Due to clinical scan, it is not easy to obtain many acquisitions. For one clinical acquisition, we defined the standard derivation (SD) of each voxel in the mean image $\bar{x}$ as:

$$\mathrm{SD} = \sqrt{\frac{1}{N-1}(x_i - \bar{x})^2}. \tag{11}$$

where $\overline{x} = \frac{1}{N} x_i$, with x_i stand for the activity of one voxel in the frame i, and N stand for the total number of frame.

III. Results

The NEMA NU-4 2008 IQ phantom image reconstructed by FBP and further denoised with Gaussian filter (GF), HYPR filter (HYPR) and CIGF (from left to right: frame1, 10 and 20) are shown in figure 1. It is clearly seen that the FBP approach results in very noisy images, while Gaussian filter somewhat reduces the noise levels at the expense of smoothes the small structure. By comparison, the images using the HYPR and proposed CIGF method exhibit clearly improved images. In particular, the 1.25 mm holes are readily visualized for both HYPR and CIGF.

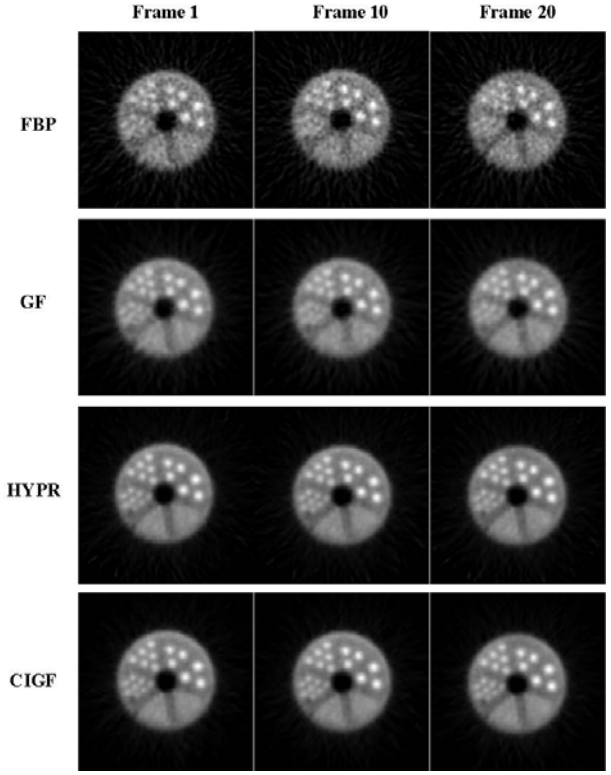

Fig. 1. The NEMA NU-4 2008 phantom image reconstructed by FBP and denoising with Gaussian filter (GF), HYPR filter (HYPR) and CIGF (from left to right: frame1, 10 and 20).

The mean and standard derivation (SD) of different methods (from top to bottom: FBP, GF, HYPR and CIGF) for each voxel through the profile is shown in figure 2.This includes mean images (left) and profiles with error bars indicating both mean and standard derivation (SD). The error bar for FBP approach is much larger than other methods. Both HYPR and CIGF have similar mean value.

To give a more clear illustration on the SD, the SD values for HYPR and CIGF are shown in figure 3. It is clearly seen the proposed CIGF method performs much better than HYPR in terms of SD.

Acknowledgment

In this work, we proposed a composite image guided filtering technique for dynamic PET denoising to enable quantitatively enhanced time frames. The proposed CIGF is considerably effective and has great potential to process data with high noise levels for dynamic PET scans.

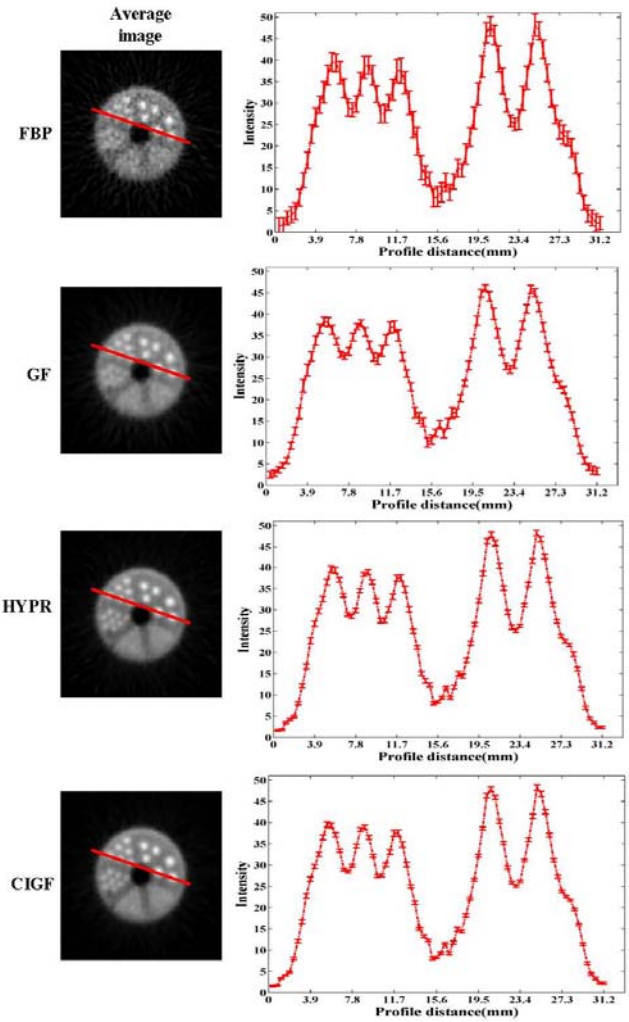

Fig. 2. The mean image (left) and profiles through the mean image(right) as obtained for images filtered by different methods. Profiles show the mean values, and the SD as error bars.

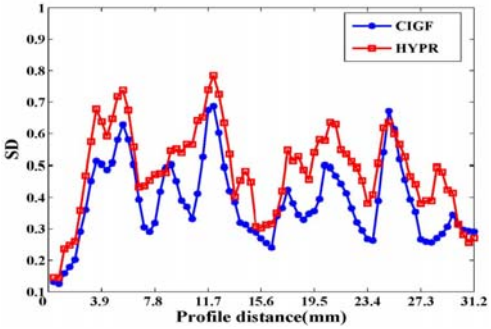

Fig. 3. The SD of each voxel through the profile of images filtered by CIGF and HYPR.

REFERENCES

[1] A. Rahmim and H. Zaidi, PET versus SPECT: strengths, limitations and challenges, Nucl Med Commun, vol. 29, (no. 3), pp. 193-207, 2008.

[2] Leahy, R.M. and J. Qi, Statistical approaches in quantitative positron emission tomography, Statistics and Computing, vol. 10, (no. 2), pp. 147-165, 2000.

[3] Reader, A.J. and H. Zaidi, Advances in PET image reconstruction, PET Clinics, vol. 2, (no. 2), pp. 173-190, 2007.

[4] Mumcuoglu, E.Ü., R.M. Leahy and S.R. Cherry, Bayesian reconstruction of PET images: methodology and performance analysis, Physics in medicine and Biology, vol. 41, (no. 9), pp. 1777, 1996.

[5] Nuyts, J., et al., A concave prior penalizing relative differences for maximum-a-posteriori reconstruction in emission tomography, Nuclear Science, IEEE Transactions on, vol. 49, (no. 1), pp. 56-60, 2002.

[6] Vunckx, K., et al., Evaluation of three MRI-based anatomical priors for quantitative PET brain imaging, Medical Imaging, IEEE Transactions on, vol. 31, (no. 3), pp. 599-612, 2012.

[7] Lu, L., et al., Anatomy-guided brain PET imaging incorporating a joint prior model, in Biomedical Imaging (ISBI), 2014 IEEE 11th International Symposium on, pp. 959-962, 2014

[8] Rahmim, A., J. Tang and H. Zaidi, Four-dimensional (4D) image reconstruction strategies in dynamic PET: beyond conventional independent frame reconstruction, Medical physics, vol. 36, (no. 8), pp. 3654-3670, 2009.

[9] Lu, L., et al., 3.5 D dynamic PET image reconstruction incorporating kinetics-based clusters, Physics in medicine and biology, vol. 57, (no. 15), pp. 5035, 2012.

[10] Wang, G. and J. Qi, PET image reconstruction using kernel method, in Biomedical Imaging (ISBI), 2013 IEEE 10th International Symposium on, pp. 1162-1165, 2013.

[11] Mistretta, C.A., et al., Highly constrained backprojection for time‐resolved MRI, Magnetic resonance in medicine, vol. 55, (no. 1), pp. 30-40, 2006.

[12] Christian, B.T., et al., Dynamic PET denoising with HYPR processing, Journal of Nuclear Medicine, vol. 51, (no. 7), pp. 1147-1154, 2010.

[13] Floberg, J.M., et al., Improved kinetic analysis of dynamic PET data with optimized HYPR-LR, Medical physics, vol. 39, (no. 6), pp. 3319-3331, 2012.

[14] He, K., J. Sun and X. Tang, Guided image filtering, in Computer Vision–ECCV 2010, Springer Berlin Heidelberg, pp. 1-14, 2010.

[15] He, K., J. Sun and X. Tang, Guided image filtering, Pattern Analysis and Machine Intelligence, IEEE Transactions on, vol. 35, (no. 6), pp. 1397-1409, 2013.

[16] Draper, N.R. and H. Smith, Applied regression analysis 2nd ed, 1981.

[17] Lu, L., et al., Performance evaluation of the Inveon PET Scanner using GATE based on the NEMA NU-4 Standards, IEEE Nuclear Science Symposium and Medical Imaging Conference (NSS/MIC), pp. 1-4, 2013.